



A Model for Estimating Total Parasite Load in Falciparum Malaria Patients

MIKE B. GRAVENOR*[†], ALUN L. LLOYD[‡], PETER G. KREMSNER[§], MICHEL A. MISSINOUS[§], MIKE ENGLISH[†], KEVIN MARSH^{||} AND DOMINIC KWIATKOWSKI[†]

[†]*Department of Paediatrics, Institute of Molecular Medicine, John Radcliffe Hospital, Oxford, U.K.*,
[‡]*Program in Theoretical Biology, Institute for Advanced Study, Einstein Drive, Princeton, NJ 08540, U.S.A.* [§]*Medical Research Unit, Albert Schweitzer Hospital, Lambaréné, Gabon and Department of Parasitology, Institute of Tropical Medicine, University of Tübingen, Germany and* ^{||}*Centre for Geographic Medicine Research, Coast, KEMRI/Wellcome Trust Laboratories, P.O. Box 230, Kilifi, Kenya*

(Received on 21 September 2001, Accepted in revised form on 19 February 2002)

We describe an age-structured mathematical model of the malaria parasite life cycle that uses clinical observations of peripheral parasitaemia to estimate population dynamics of sequestered parasites, which are hidden from the clinical investigator. First, the model was tested on parasite populations cultured *in vitro*, and was found to account for ~72% of the variation in that sub-population of parasites that would have been sequestered *in vivo*. Next, the model was applied to patients undergoing antimalarial therapy. Using individual data sets we found that although the model fitted the peripheral parasite curves very well, unique solutions for the fit could not be obtained; therefore, robust estimates of sequestered parasite dynamics remained unavailable. We conclude that even given detailed data on individual parasitaemia, estimates of sequestered numbers may be difficult to obtain. However, if data on individuals undergoing similar therapy are collected at equal time intervals, some of these problems may be overcome by estimating specific parameters over groups of patients. In this manner we estimated sequestered parasite density in a group of patients sampled at identical time points following antimalarial treatment. Using this approach we found significant relationships between changes in parasite density, age structure and temperature that were not apparent from the analysis of peripheral parasitaemia only. © 2002 Elsevier Science Ltd. All rights reserved.

Introduction

Malaria parasites injected into the human host by mosquitoes initially migrate to the liver. These parasites (sporozoites) invade liver cells and undergo asexual reproduction, releasing a

large number of merozoites into the bloodstream. There, each merozoite invades a red blood cell and reproduces asexually. After approximately 48 hr the erythrocyte ruptures releasing daughter parasites that quickly invade a fresh erythrocyte to renew the cycle. The 'erythrocyte cycle' maintains infection and directly generates disease symptoms.

An important characteristic of *Plasmodium falciparum*, the most virulent malaria parasite, is

*Corresponding author. Tel.: +44-01635-578411; fax: +44-01635-578844. Present address: Institute for Animal Health, Compton, Berkshire, RG20 7NN, UK.

E-mail address: michael.gravenor@bbsrc.ac.uk (M.B. Gravenor).

sequestration. At the half-way point of parasite development, the infected erythrocyte leaves the circulating blood and binds to endothelium in the microvasculature where the cycle is completed. Daughter parasites released at erythrocyte rupture re-enter the circulation and invade a fresh erythrocyte. A measurement of *P. falciparum* parasitaemia taken from a blood smear therefore samples young parasites only. It is difficult to relate this measure to the total parasite density. In many cases a population of parasites develops in synchrony. A low peripheral parasitaemia may reflect low or high total parasite numbers depending on the level of synchrony and the mean age of the parasite population. Peripheral parasitaemia therefore tends not always to be a good correlate of clinical parameters.

It is difficult to form a reliable picture of the response to antimalarial therapy without knowing the behaviour of the sequestered parasite population. Since antimalarial drugs are known to act preferentially on different stages of parasite development, it is conceivable that a drug that quickly cleared parasites from the peripheral blood might effect slower clearance of sequestered parasites. This is of particular importance since parasite sequestration is considered central to the pathology of severe malaria. White *et al.* (1992) showed that mathematical models can be used to describe patterns of parasite sequestration. Gravenor *et al.* (1998) presented a simple method for generating estimates of the level of sequestered infection from observed peripheral parasitaemia in children undergoing drug treatment. Here, we describe a general approach to modelling the age structure of *P. falciparum* that can be adapted to suit the particular data set that is to be analysed. We provide a test of the approach using *in vitro* populations of parasites, apply the model to two detailed clinical data sets and use the model predictions to investigate the relationship between patient temperature and total parasite density.

Materials and Methods

A GENERAL AGE-STRUCTURED MODEL OF THE ERYTHROCYTE CYCLE

Figure 1 illustrates the intraerythrocytic life cycle of *P. falciparum*, which lasts approximately

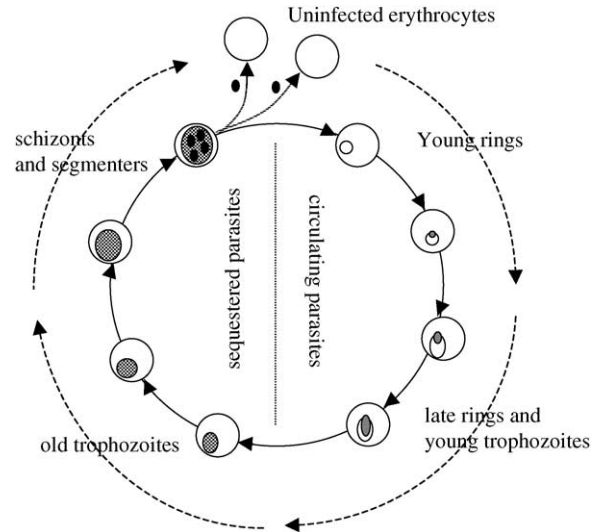


FIG. 1. The mathematical model of the life cycle is based on a finite number of compartments (here depicted as circles), each representing an equal duration of development time. In the above example, there are eight Compartments and since the parasite life cycle is 48 hr, each compartment represents 6 hr. Parasites can often be aged on appearance. Four commonly used morphological stages are young rings, late rings/young trophozoites, old trophozoites and schizonts/segmenters. In this model, these are each represented by two compartments (though more can be used). In an infected individual, parasites in approximately the first half of the cycle (young rings–young trophozoites) circulate freely and can be seen in the peripheral blood, while all other parasites sequester in the deep vasculature (old trophozoites–segmenters) and cannot be detected.

48 h. In our model, we divide the cycle into a number of successive *compartments*. One of the critical problems to be discussed later is how to decide upon the number of parasite compartments in the model, but a useful starting point is the morphological appearance of the parasite as shown in the figure. Immediately after the erythrocyte invasion, the parasite has the appearance of a ‘ring’, after about 12 hr it gradually adopts a more solid appearance and is known as a ‘young trophozoite’ (or late ring). After 24 hr the trophozoite continues to grow and finally it becomes a ‘schizont’ or ‘segmenter’ for the last 12 hr or so of the cycle, before rupturing to release daughter parasites which infect other erythrocytes. In the infected individual *in vivo*, the parasite-infected erythrocytes circulate freely in the bloodstream during the first half of the life cycle, but at about 24 hr into

the cycle the mature trophozoites sequester in deep blood vessels and consequently disappear from the peripheral blood. The model described in this paper divides the 48 hr life cycle into a finite number of compartments of equal duration. For example, Fig. 1 illustrates a model with eight compartments, each of 6 hr duration, such that compartments 1 and 2 roughly correspond to young rings, compartments 3 and 4 to late rings and early trophozoites, compartments 5 and 6 to mature trophozoites and compartments 7 and 8 to schizonts or segmenters. In the following sections we consider how to choose the number of compartments and other parameters of the model.

This paper deals specifically with the issue of parasite dynamics in patients receiving antimalarial drug therapy. In these circumstances, the population dynamics are dominated by high parasite death rates that can reduce parasitaemia by orders of magnitude within 48 hr, and parasite clearance is approximately first order (declines exponentially). These death rates are determined by the drug in use, and vary considerably with the age of the parasite. A natural choice to describe the cycle is a Markov chain, which has a number of transition compartments that represent parasite age, hence a developing parasite passes through each compartment in sequence at a specific rate. In addition to these transition rates, the parameters of the model are death rates at each compartment (i.e. age dependent). This approach contrasts with more complicated models that describe parasite population dynamics during untreated *P. falciparum* infections (Gravenor *et al.*, 1995; Gravenor & Kwiatkowski, 1998; Kwiatkowski & Nowak, 1991; Molyneaux *et al.*, 2001).

The model is used to simulate the behaviour of a parasite population over time from the starting point of any initial distribution of parasites across the compartments of the model (the age structure of the parasite population at the onset of drug treatment). The rate of change of the average numbers of parasites in each of the x compartments is as follows:

$$\frac{dn_{1(t)}}{dt} = R\lambda n_{x(t)} - (\lambda + \mu_1)n_{1(t)}$$

and

$$\frac{dn_{i(t)}}{dt} = \lambda n_{i-1(t)} - (\lambda + \mu_i)n_{i(t)}$$

for $i = 2, \dots, x$.

The average duration of the cycle is 48 hr, hence if the time period of transition between each compartment is equal, $\lambda = x/48 \text{ hr}^{-1}$. R is the number of daughter intracellular parasites produced at the end of each cycle. Key parameters of the model (to be estimated from the data) are parasite death rates (μ_i), which are age dependent and can differ between each compartment. Sequestration can be defined to occur at a particular point of the cycle (or over a range of compartments); therefore, the age structure of both the peripheral and sequestered parasites can be described. In the models considered here, sequestration occurs at the half-way point.

The number of compartments x is chosen to reflect the distribution of cycle lengths appropriate for *P. falciparum* and has an important impact on the growth rate of the model (Saul, 1998, Gravenor & Lloyd, 1998), which can be unrealistic if x is too small. It can be shown that the distribution of cycle lengths in the x -compartment model is described by a gamma distribution, with mean 48 hr and standard deviation $48/\sqrt{x}$ (Lloyd, 2001a, b). At the extremes, one compartment represents an exponential and highly variable distribution of generation times, whilst for $x \rightarrow \infty$, all parasites complete their cycle in exactly 48 hr. The effect of varying the number of compartments is most marked at low values of x . The aim of this approach is to allow some change in the level of synchrony of the population due to small differences in generation times. Discrete models have been used for *P. falciparum* population dynamics (White *et al.*, 1992; Hoshen *et al.*, 2000; Molyneaux *et al.*, 2001) in which no variation in cycle length occurs (a situation that can be modelled here as $x \rightarrow \infty$).

The data available to fit the model are usually sparse, allowing estimation of only a few parameters. For a multicompartment model certain parameter values must therefore be assumed equal across several model

compartments. Here we introduce the term *domain* to describe several compartments that have been grouped together, in the sense that they are assigned identical parameter values. The number of free parameters (parasite death rates) is dictated by the particular data set, and for the data analysed in this paper, the number of domains should ideally be determined by the developmental specificity of the drug in use. Similarly, the initial age structure of the parasite population cannot be estimated over all compartments, and must be estimated as a distribution over domains (that may differ from those defined for drug specificity).

Note that if the initial parasite age structure is estimated for y domains, assuming a distribution (e.g. uniform) over the compartments within each domain, this is not equivalent to reducing the Markov chain to y compartments. There is a distinction between the number of compartments in the underlying model, which is determined on mathematical grounds, and the number of domains the compartments are grouped into. The number of compartments x largely determines the model behaviour: it should reflect the true variation in parasite generation time. A domain is a group of compartments that share identical parameter values. How these mathematical compartments are grouped into domains is a practical constraint. There is a trade-off between fine tuning of the model (where the ideal solution may be to have many domains, each corresponding to a very specific stage of the life cycle) and the problem of parameter estimation from sparse data (which may be intractable if the number of domains is large).

PARAMETER ESTIMATION

Parameters can be estimated from observations on changes in the number of parasites in each developmental stage over time. Clinical data describe only the total peripheral parasitaemia, hence the sum of the model population in those compartments representing peripheral parasitaemia (the first half of the compartments) was fitted to the data. Parameters and initial conditions were estimated with an algorithm that minimizes the least-squares difference between

the model and data [NAG routine E04JAF (1992), Numerical Algorithms Group Ltd., Oxford, U.K.].

If possible all free parameters and initial conditions are estimated from each patient. This approach takes into account different responses to therapy and in particular the initial distribution of parasites, which will vary considerably. When data are scarce, the algorithm may fail to find a unique solution for the parameter set. A non-unique fit is obtained when the sum of squares for the fit to the data has more than one local minimum [the exact criteria are specified by NAG routine E04JAF (1992), Numerical Algorithms Group Ltd., Oxford, U.K.]. This means the data can be equally well described by different sets of parameters. If this occurs, we suggest that an alternative approach is to estimate parasite death rates as averages over a group of patients, whilst estimating an initial age structure unique to each patient (Gravenor *et al.*, 1998). For this procedure, bootstrap estimates of mean parasite death rates are obtained. A large number of mean parasite clearance profiles are sampled at random from the full data set (by sampling individuals with replacement), and the model is fitted to each mean profile in turn. From the set of best-fitting parameter values we obtain an estimate of the mean value for the parasite death rates, with associated confidence interval (not dependent on an assumed normal distribution for the data). Then, to estimate sequestered dynamics for each patient, the mean parasite death rates are included in the model as constants (or ranges), leaving only a unique initial parasite age structure to be estimated for each individual patient. This method can only be used if the same drug regime is used for each patient, and is best applied if parasitaemia is sampled at the same time intervals for each patient (such structured data ensure a mean profile reflects an individual profile).

TEST OF MODEL USING *IN VITRO* DATA

In vivo, the goodness of fit of the model can only be assessed by how well it reproduces the clearance of peripheral parasites. There is no direct way of evaluating the model predictions of sequestered dynamics in a clinical data set.

However, since parasites of all ages can be observed in culture, we used *in vitro* data for an assessment of the model performance.

Population changes in ten cultures of *P. falciparum* (Trager & Jensen, 1976) were monitored with thin blood smears. The cultures were initialized at low density (<1% erythrocytes infected) to minimize density-dependent effects and maintain a first-order process. Each culture was studied over the exponential growth phase lasting 72–96 hr. The number of parasites in each of five developmental stages was counted every 12 hr. These categories were identified by morphology and corresponded to young rings (0–12 hr), old rings (12–19 hr), young trophozoites (19–27 hr), old trophozoites (27–41 hr) and segmenters (41–48 hr).

The model was fitted to the time series of young parasites only (young and old ring categories combined), mimicking the process of fitting the model to clinical parasitaemia. The fit was then used to predict the behaviour of the older parasites. Unlike clinical situations, we were able to compare model predictions of older parasite dynamics to the data. Note that the model was fitted to parasite growth rather than clearance curves. However, the processes of changes in age structure are the same assuming both are first order. In addition, at low density the parasite death rates were very low, which reduced the crucial values to be estimated to R and an initial age structure.

CLINICAL DATA

The model was applied to two sets of clinical data. First, a study of quinine therapy in Kenyan children, where 69 children were monitored for parasitaemia until a clear blood film was found. Over the first 48 hr on average ten samples per patient were taken, providing a detailed set of data at a sampling frequency that is far in excess of standard clinical practice. Since sampling was carried out at irregular intervals, different for each patient, we refer to this set as ‘detailed irregular sampling’. Three example clearance curves are given in Fig. 2(a). Due to irregular sampling, the mean clearance profile does not provide a good indication of an individual clearance curve.

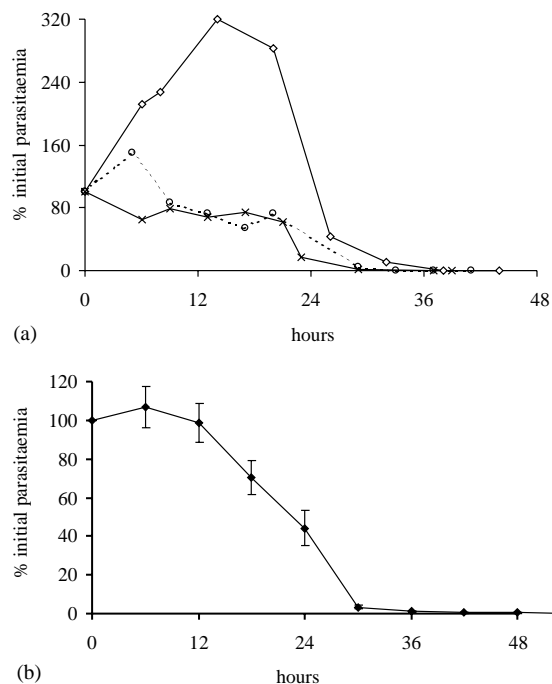


FIG. 2. Clinical data. (a) Detailed irregular sampling. Three examples of individual parasite clearance curves from Kenyan trial of quinine in 69 patients. (b) Structured sampling. Parasite clearance curve averaged (\pm S.E.) over 26 patients from Gabon. Parasitaemia sampled every 6 hr. Parasitaemia expressed as % of initial peripheral parasite density, hours are post-onset of treatment.

The second data set comprised the first 26 children of a larger study from Gabon (Lell *et al.*, 2001). Each patient received quinine therapy and parasitaemia was recorded at the onset of treatment and then every 6 hr until no parasites were detected in the blood. We refer to these data as ‘structured sampling’. The mean clearance profile is given in Fig. 2(b). Temperature recordings were taken at hourly intervals.

Results

NUMBER OF MODEL COMPARTMENTS AND DOMAINS

Figure 3 compares the behaviour of models with different numbers of compartments. The simulations show the number of parasites ‘sequestered’ (those in the second half of development) if all parasites are initially less than 12 hr old. Using a model with a small number of compartments ($x = 4$) there is considerable variation in parasite development times, hence a proportion of parasites sequester

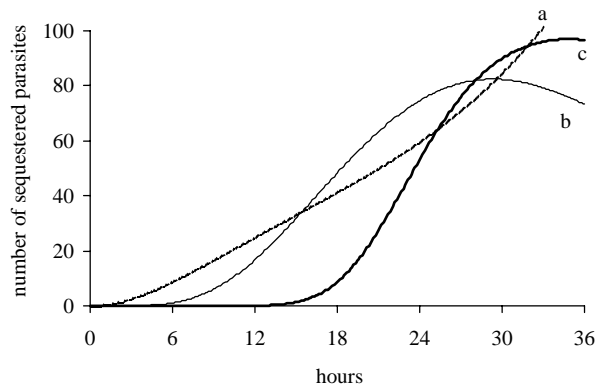


FIG. 3. Effect of number of compartments included in the model on time to sequestration: (a) 4-compartment model, (b) 20-compartment model and (c) 48-compartment model. Hundred parasites are introduced into the first compartment of each model at $t = 0$. Sequestration occurs between the compartments at the midpoint of the cycle. $\mu_i = 0$.

very quickly, and the overall process of sequestration is gradual. As more compartments are added to the model the time to sequestration is less variable ($x = 20$). *In vitro* data suggest that binding of maturing *P. falciparum* to endothelium occurs with a step sigmoidal function (Gardner *et al.*, 1996). This was reproduced with a 48-compartment model, each conveniently representing 1 hr of development. The coefficient of variation for the parasite generation times is therefore 14%, and an initially synchronous population will gradually become asynchronous

over several cycles in the absence of external influences.

The maximum number of parameter domains to group the model compartments was found by trial and error. The number was chosen such that a unique fit for the model to the data was obtained. For the clinical data, it appeared that two distinct death rates could be estimated, alongside four values for the initial age distribution. Quinine was used in both studies. Since young and mature parasites are relatively quinine resistant compared to the middle part of the cycle (Geary *et al.*, 1989), we assigned μ_1 to the first and last 12 hr and μ_2 to the intermediate compartments of the model. The initial age distribution was estimated over four domains: 0–12, 12–24, 24–36 and 36–48 hr. In each model we used a value of R between 10 and 12 as a fixed parameter (Gravenor *et al.*, 1995). To explore the effect of modifying some of these assumptions on the model performance we considered three further models: μ_2 applying to 24–48, 8–40 and 4–44 hr. A schematic of the structure of the specific model used for analysing the clinical data is given in Fig. 4.

For the *in vitro* data since all death rates were very low, it was possible to estimate five values for the initial age distribution in addition to R . The five initial age domains covered compartments: 0–12, 12–19, 19–27, 27–41, 41–48.

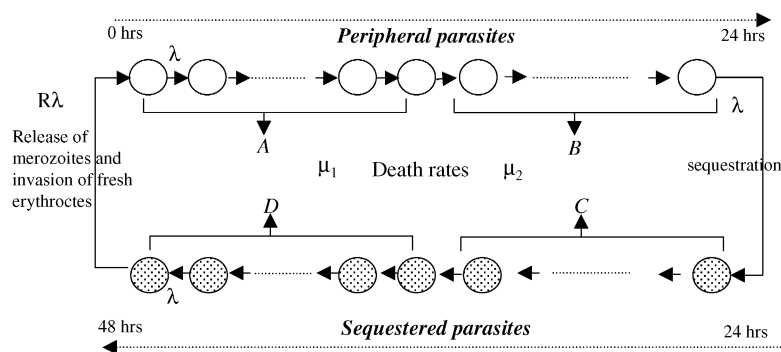


FIG. 4. Outline of specific model used for analysis of clinical data. The underlying Markov chain has 48 compartments, each an average duration of 1 hr. The parasites inhabit red blood cells and circulate in the peripheral blood for the first 24 hr of the cycle (white circles), then sequester in the microvasculature for the second 24 hr (shaded circles). The parameters of the model apply across domains of parasite compartments. Parasite death rates are estimated in two domains: μ_1 for parasites in the first and last compartments of the cycle (A and D) and μ_2 for the intermediate compartments (B and C). Estimates of initial population age structure are made for four different domains (A–D) each comprising 12 compartments. The initial population structure within these compartments is assumed uniform. $\lambda = 1 \text{ hr}^{-1}$, $R = 10\text{--}12$.

PERFORMANCE OF MODEL USING *IN VITRO*
POPULATIONS

Examples of the *in vitro* test of the model are provided in Fig. 5. In the ten populations, the fit of the model to the younger ('peripheral') parasite sub-population generated an average r^2 (% variation in the data explained by the model) of over 80%. When compared to the data, the corresponding r^2 for the predictions of the older ('sequestered') sub-population was 72%. Figure 5(a) shows that a good fit to the peripheral population ($r^2 = 95\%$) yielded a good fit to the sequestered population ($r^2 = 90\%$). The fit was not always so good, for example in Fig. 5(b), the sequestered density tended to be overestimated ($r^2 = 69\%$) despite an excellent fit to the peripheral data ($r^2 = 99\%$). Figure 5(c) gives a clue to where the model may be less accurate. This particular culture had a highly synchronized population. Since in this case the initial conditions of the model are averaged over fairly wide age groups (five domains), the model struggled to fit the peripheral data ($r^2 = 60\%$). Interestingly, r^2 for the sequestered population remained high (86%).

CLINICAL DATA SET I

With these data we estimated all model parameters on an individual patient basis. At first glance, the model appeared to provide an excellent description of the parasite population dynamics. Figure 6 shows two examples of the model fit and predicted sequestered parasite density. Over all 69 patients, the variation in the data explained by the model was on average 91%. Following the *in vitro* results, the goodness of fit suggested that the model would provide useful descriptions of the sequestered population. However, although the algorithm found a combination of parameters that gave a close fit to the data, this combination was not unique and different combinations of widely ranging parameters could be found which fitted equally well. A unique fit to the data could not be found in over 30% of cases. This means that the confidence ranges for parameter estimates were far too wide to be of use in predicting sequestered numbers.

The presence of multiple solutions for the model fit was expected after examining the relative values of μ_1 and μ_2 between individuals. From pharmacological studies it is known that

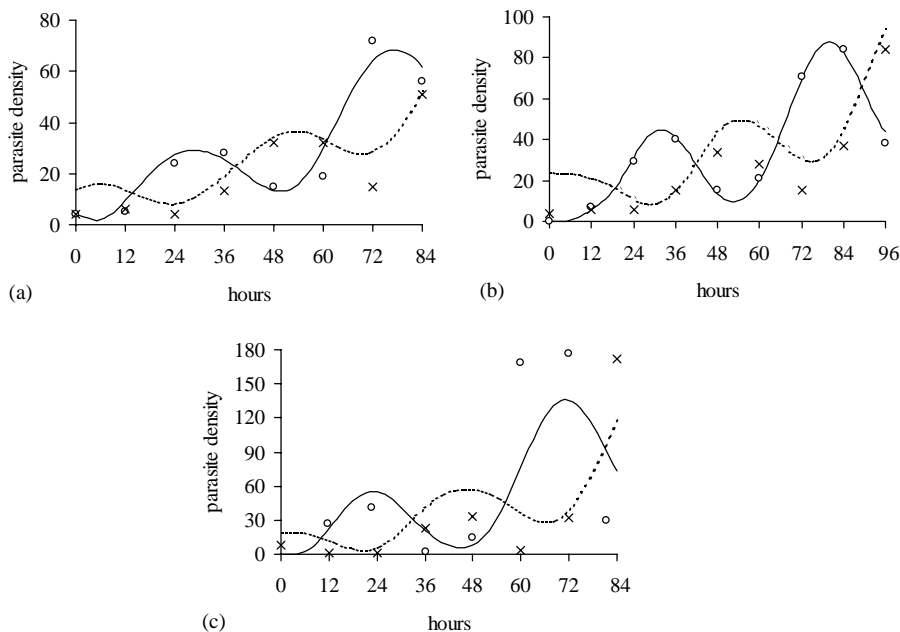


FIG. 5. Examples of model performance using *in vitro* populations. Data on parasites aged 0–19 hr combined (circles) were used to predict changes in the population of parasites aged 19–48 hr (crosses). Fit of model is given by solid line. Predictions of 'sequestered' population is given by dotted line. Goodness-of-fit statistics is given in text.

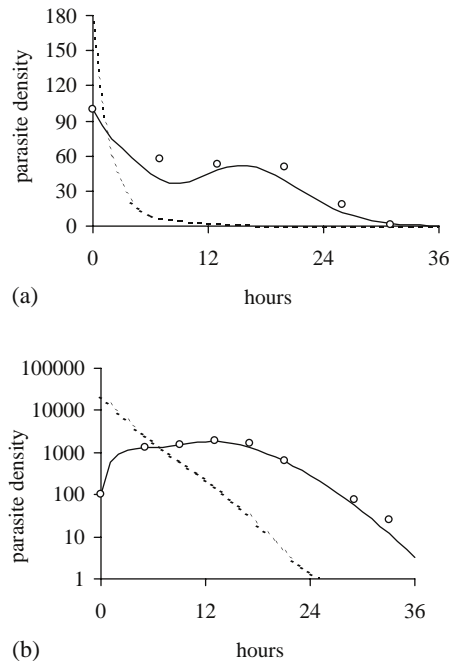


FIG. 6. Fit of the model to clinical data set 1. Clinical data given by circles, solid line denotes fit of model to clinical data, dotted line predicted sequestered parasites. Parasite density plotted as a % of peripheral parasitaemia at $t = 0$. (a) r^2 for peripheral parasitaemia = 96%, estimated parameters: $\mu_1 = 0.0$, $\mu_2 = 0.54$, $R = 12$, estimated initial age structure (0–12, 12–24, 24–36, 36–48 hr): 100, 0, 172, 2. (b) $r^2 = 98\%$, parameters: $\mu_1 = 0.17$, $\mu_2 = 0.43$, $R = 12$, estimated initial age structure: 100, 0, 20 745, 584.

$\mu_1 < \mu_2$ (reflecting the relative resistance of ring and schizont compared to the mid cycle). Furthermore, since the patients received the same drug regime, values for each death rate should not vary greatly between individuals. Contrary to these expectations, the mean value of μ_1 (2.63) was greater than μ_2 (1.36) and between patient standard deviations considerably exceeded the means (12.71 and 5.81, respectively).

To illustrate the problem of multiple solutions we considered the data in Fig. 6(a) and found a different set of parameters (by initializing the estimation algorithm at a different starting point) that gave similar fits to the data, but predicted very different sequestered population dynamics. The first estimates suggest, as expected, that mid-cycle parasites are relatively much more sensitive to the drug ($\mu_1 = 0$, $\mu_2 = 0.54$) and at onset of treatment there are two broods of parasites in the ratio 1 peripheral

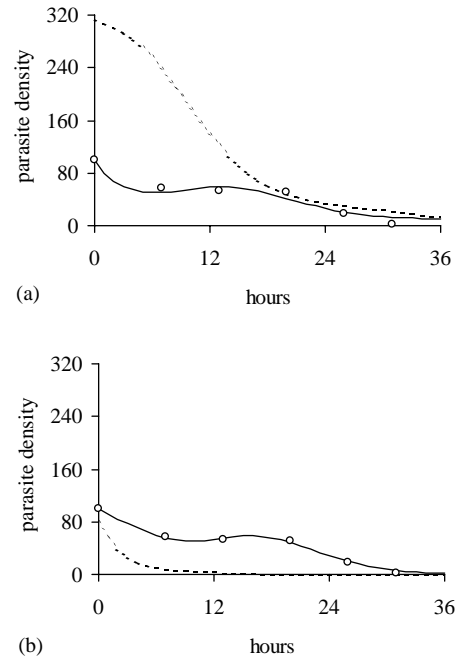


FIG. 7. Multiple solutions for fit to data set 1. Clinical data as in Fig. 6(a) (circles), solid line denotes fit of model to clinical data, dotted line denotes predicted sequestered parasites. Parasite density plotted as a % of peripheral parasitaemia at $t = 0$. Parameters obtained by initializing estimation algorithm with differing starting values. (a) r^2 (fit to peripheral parasitaemia) = 97%, parameters: $\mu_1 = 0.4$, $\mu_2 = 0.02$, $R = 12$, estimated initial age structure (0–12, 12–24, 24–36, 36–48 hr): 100, 0, 312, 3. (b) $r^2 = 99\%$, parameters: $\mu_1 = 0.0$, $\mu_2 = 0.37$, $R = 12$, estimated initial age structure: 100, 0, 76, 3.

to 1.7 sequestered. Predicted sequestered dynamics show a simple exponential decline [Fig. 6(a)]. However, the data can equally be described [Fig. 7(a)] with parameters reflecting greater sensitivity of ring compartments ($\mu_1 = 0.4$, $\mu_2 = 0.02$) and an initial ratio of 1 peripheral to over 3 sequestered parasites. The corresponding sequestered dynamics differ significantly, having a slower decline from the initially large sequestered mass. It is possible in such cases to impose a constraint on the fit based on the pharmacological information such that μ_1 must be less than μ_2 . However, Fig. 7(b) shows that the same data could also be well described by simultaneously reducing the death rates and the initial sequestered mass. This led to an estimate of sequestered parasitaemia 50% of that in Fig. 6(a).

Similar problems were also encountered when comparing the predictions from models with

differing domains for μ_1 and μ_2 (μ_2 applying to 8–40, 4–44 or 24–48 hr). Since these data could be described with different parameter sets or different models, that generated very different predictions of sequestered dynamics, the estimates of total parasite density were unreliable.

CLINICAL DATA SET 2

On an individual basis, these data were not collected as frequently as data set 1, hence multiple solutions were also present when all parameters were estimated on an individual basis. However, parasite density was always recorded at equal time intervals, and each patient received exactly the same drug regime. This allows good estimates of the average response to therapy to be calculated, and mean values of μ_i to be obtained over all patients. From the average clearance curve [Fig. 2(b)], bootstrap estimates of parasite death rates were [mean (hr^{-1}) \pm S.E.] $\mu_1 = 0.035 \pm 0.08$, $\mu_2 = 0.59 \pm 0.3$. The parasite death rates for each patient were then fixed at the means to allow estimation of unique starting age distributions. Note that the fit of the model to the average clearance curve generated a unique solution for μ_1 and μ_2 , and that unique solutions for the initial age-distribution in each patient were then obtained.

An example of the model fit is given in Fig. 8(a). Here, the full parasite population was largely confined to the peripheral blood at the onset of treatment. Peripheral parasitaemia remained high for the first few hours due to bursting of a small number of schizonts immediately after treatment. The delay in clearance of sequestered parasites was due to the large number of parasites in the 12–24 age compartment, a proportion of which were able to sequester before being killed off by the drug treatment. Figure 8(b) illustrates a case with similar numbers of peripheral and sequestered parasites at the onset of treatment. A rise in peripheral parasitaemia followed bursting of small numbers of late compartment parasites. A smooth decrease in sequestered density occurred since initially there were no parasites estimated in the 12–24 age domain and the majority of sequestered parasites were aged

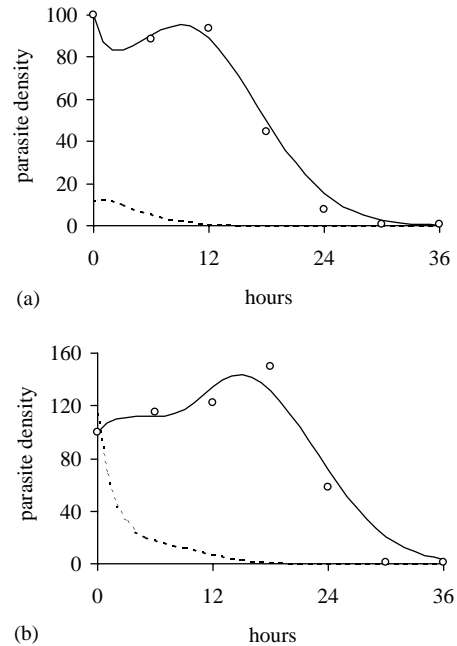


FIG. 8. Fit of the model to data set 2. Clinical data given by circles, solid line denotes fit of model to clinical data, dotted line denotes predicted sequestered parasites. Parasite density plotted as a % of peripheral parasitaemia at $t = 0$. (a) $r^2 = 99\%$, parameters: $\mu_1 = 0.035$, $\mu_2 = 0.59$, $R = 12$, estimated initial age structure (0–12, 12–24, 24–36, 36–48 hr): 57, 43, 0, 12. (b) $r^2 = 97\%$, parameters: $\mu_1 = 0.035$, $\mu_2 = 0.59$, $R = 12$, estimated initial age structure: 100, 0, 100, 12.

24–36 hr. Over all patients, the observed average parasitaemia at the onset of treatment was $94\,000\ \mu\text{l}^{-1}$ (± 9300). The estimated average number of sequestered parasites (relative to $1\ \mu\text{l}$ blood) was $53\,000$ ($\pm 12\,000$).

Exploring other model structures, we found that the two models which assumed μ_2 to act over the domains 8–40 or 4–44 hr tended to give slightly higher estimates of sequestered load, but the predictions for individual patients were highly correlated. The model with less realistic death rate domains (μ_2 acting over the period 24–48 hr) was rejected. When fitting this model to the averaged or individual data, multiple solutions were present for the parameters and significantly less variation in observed parasitaemia was accounted for.

RELATIONSHIP BETWEEN SEQUESTERED PARASITE DENSITY AND TEMPERATURE

Using the results from data set 2 we investigated the relationship between parasite load and

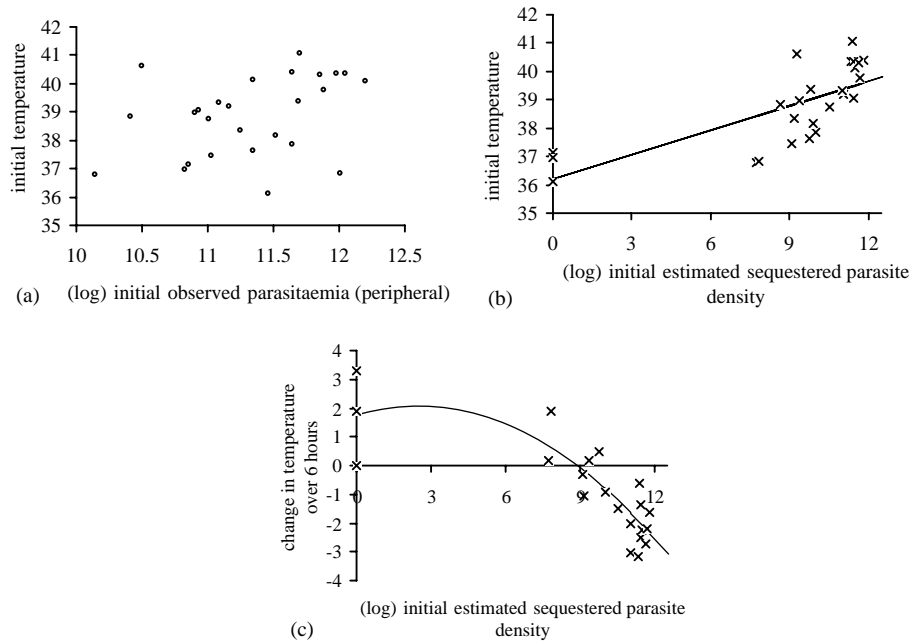


FIG. 9. Relationship between temperature and parasite population dynamics. (a) Temperature at the onset of treatment vs. observed initial parasitaemia [specifically, $\log_e(\text{parasites} + 1)$]. $r^2 = 0.12$, $p = 0.1$. (b) Temperature vs. estimated initial sequestered parasite density. $r^2 = 0.54$, $p < 0.001$, best fitting regression line $36.2 + 0.29x$. (c) Change in temperature (Δt) over first 6 hr of treatment vs. initial sequestered parasite density. $r^2 = 0.73$, $p < 0.001$, best fitting regression line $1.75 + 0.27x - 0.05x^2$. If the very low numbers of sequestered estimates are removed, the highly significant relationships remain: (b) $31.82 + 0.71x$, (c) $7.42 - 0.82x$.

temperature. There was no observed relationship between temperature and peripheral parasitaemia over the first 6 hr of treatment [Fig. 9(a)]. Sequestered (and total) parasite load on admission was significantly correlated with initial temperature ($p < 0.001$) [Fig. 9(b)]. Sequestered load was also significantly related to the change in temperature over the first 6 hr of treatment [$p < 0.001$, controlling for initial temperature, Fig. 9(c)]. Note that only the slopes of the fitted equations (not the significance of the relationships) were dependent on the very low sequestered density estimated in three patients.

Discussion

A reliable clinical method of estimating the total parasite load for *P. falciparum* infections is unavailable. Possible methods could involve finding good correlates with non-sequestering by-products of infection, or substances that respond in a predictable way to overall parasite load. Our approach is based on developing mathematical models that capture the essential

parasite population dynamics during drug therapy, and estimating their parameters from clinical data.

A general framework for modelling the parasite population is suggested, and in practice the complexity of the model was determined by the amount of data available. Even though data sampling was relatively frequent, there was insufficient data to fit a detailed model. Initial age structure was estimated as a distribution over four 12-hr domains of the life cycle, and only two distinct death rates were permitted. When choosing the exact point for the parameters to act, prior information may be available or it may be possible to differentiate between models on the basis of model fit. Based on pharmacological studies of quinine, models were preferred with parasite death rates being highest during the middle part of the parasite cycle. Hence the model with μ_1 acting at 0–24 hr and μ_2 at 24–48 hr did not fit well, due to the grouping together of parasites that have very different death rates. Models with more subtle differences may be indistinguishable and it may

be important to draw conclusions on sequestered estimates based on a range of models.

In vitro cultures were used to show that the model adequately described parasite population dynamics, and the fit to the peripheral population generated accurate estimates of changes in the density of those parasites that would have been sequestered in clinical infections. Given this performance, the application of the model to clinical data set 1 was disappointing. Even though the model fitted the peripheral parasitaemia, a range of parameter solutions existed for the same data. The range of predictions for sequestered dynamics was then too wide to be useful. This highlights the danger of relying solely on the fit to peripheral parasitaemia when making predictions about the sequestered population. The contrast with the *in vitro* data is largely due to the number of estimated parameters. Parasite death rates in culture at all ages were low, and the dynamics were largely determined by the initial age structure only. In a clinical setting, parasite death rates are very high and vary substantially with parasite age. The extra parameters led to the problem of multiple solutions for the model fit in the clinical setting, but were essential for a reasonable description of the underlying biological process.

The structure of clinical data set 2 offered an opportunity to use the same model, even though blood samples were taken less frequently. The additional assumption was that parasite death rates did not vary considerably between patients, and could be fixed at the values estimated from the average clearance curve. As expected the mean estimate of μ_2 was much higher than μ_1 , reflecting the stage specificity of quinine. With the extra degrees of freedom for the fit to individual clearance curves, unique solutions were obtained for the initial age structure in 26 patients. Initial sequestered parasite density in these patients was on average 50% that of peripheral parasitaemia, but varied considerably (range 0–166%) between patients. Although initial sequestered density was slightly more variable than peripheral parasitaemia, following treatment sequestered densities were much more uniform between patients. This may be due to a dampening effect of the drug, and the cyclical nature of parasite development: one peripheral

parasite leads to one sequestered parasite, but one sequestered parasite can generate up to many peripheral parasites. Sequestered population dynamics may be inherently less variable [e.g. Fig. 3(c)], which aids the estimation process.

Applying the model estimates to other clinical measures, we found that sequestered parasite density was related to initial temperature, and the changes in temperature over the first 6 hr of treatment. Interpreting the relationships at $t = 0$ is difficult since it is a static observation and changes in parasite number and age structure are the likely cause of fever. The model cannot be used to extrapolate backwards before treatment since parasite death rates would be unknown and very different at this time. Fever is triggered (with a time delay) by the bursting of schizonts, and tends to occur at a threshold parasite density (Kwiatkowski, 1995) (although in addition, malarial fever shows a clear circadian rhythm, Lell *et al.*, 2000). We might therefore expect high temperature on admission to reflect high parasite density and a high ratio of peripheral to sequestered parasites. Here, high fever was best predicted by a high sequestered mass combined with a high proportion of parasites aged 24–36 hr. This suggests schizont rupture occurred at a considerable time before treatment began in those patients with fever at $t = 0$. Changes in temperature over the first 6 hr (Δt) must be constrained to some extent by initial temperature. Controlling for this variable we found sequestered load remained negatively correlated with Δt . An increase in Δt was best predicted by low initial sequestered load and a high initial proportion of parasites aged 12–24 hr. This suggests that the time from schizont rupture to a peak temperature is up to 12 hr. However, the initial age structure may not be modelled in enough detail at present to accurately determine this relationship.

There are a number of simple means by which additional complexity, or different assumptions can be incorporated into this model framework. Parameters can be made time dependent (e.g. death rates decreasing exponentially after each dose) to reflect drug and treatment regime (such as mefloquine which is applied infrequently and has a long half-life). For the above data, drug treatments are given at frequent intervals and we

considered the additional difficulty in estimating parameters for such a model to outweigh the benefits of additional complexity. The use of a time delay before the drug begins to act may be appropriate. Dead parasites are likely to be involved in pathology. If an additional parameter is introduced (the rate of decay of dead sequestered parasites) the model can describe the clearance of the full sequestered mass and can be compared with histopathology data. Different approaches can be taken to estimate initial age structure. If we could assume one brood of parasites, the degree of synchrony could be described by a uniform distribution over y compartments (small y being highly synchronous). We then need only to estimate two values for the initial age distribution, the total parasite density and y . Different distributions may be more appropriate (particularly due to the high reproductive potential of the population) which would require further parameters. Similarly, if two broods were present more parameters would be introduced. If the age of peripheral parasites can be estimated (by morphology) this additional information can be exploited to improve predictions.

In vitro tests suggest that our model is an appropriate tool for assessing sequestered population density. However, experience with the clinical data showed that parameters for even a simple model cannot be estimated with confidence unless large amounts of data are available. Data collected over equal time intervals are more useful, and a sampling frequency of at least 4 hr will be needed to add more detail to the model analysed here. The method for revealing sequestered population dynamics is at an early stage, and predictions of clinical relationships should be treated with caution. However, analysis of detailed time series with this model framework offers the opportunity to explore relationships between clinical variables, the parasite population and the pathogenesis of malaria.

This work was supported by Medical Research Council Fellowships (MBG, ALL) and a Wellcome Trust Career Development Fellowship (ME). This paper is published with the permission of the director of KEMRI. We thank two anonymous referees for helpful comments.

REFERENCES

- GARDNER, J. P., PINCHES, R. A., ROBERTS, D. J. & NEWBOLD, C. I. (1996). Variant antigens and endothelial receptor adhesion in *Plasmodium falciparum*. *Proc. Natl Acad. Sci. U.S.A.* **93**, 3503–3508.
- GEARY T. G., DIVO, A. A. & JENSEN, J. B. (1989). Compartment specific actions of antimalarial-drugs on *Plasmodium falciparum* in culture. *Am. J. Trop. Med. Hyg.* **40**, 240–244.
- GRAVENOR, M. B. & KWIATKOWSKI, D. (1998). An analysis of the temperature effects of fever on the intra-host population dynamics of *Plasmodium falciparum*. *Parasitology* **117**, 97–105.
- GRAVENOR, M. B. & LLOYD, A. L. (1998). Reply to: models for the in-host dynamics of malaria revisited: errors in some basic models lead to large overestimates of growth rates. *Parasitology* **117**, 409–410.
- GRAVENOR, M. B., MCLEAN, A. R. & KWIATKOWSKI, D. (1995). The regulation of malaria parasitaemia: parameter estimates for a population model. *Parasitology* **110**, 115–122.
- GRAVENOR, M. B., BOELE VAN HENSBROEK, M. & KWIATKOWSKI, D. (1998). Estimating sequestered parasite population dynamics in cerebral malaria. *Proc. Natl Acad. Sci. U.S.A.* **95**, 7620–7624.
- HOSHEN, M. B., HEINRICH, R., STEIN, W. D. & GINSBURG, H. (2000). Mathematical modelling of the within-host dynamics of *Plasmodium falciparum*. *Parasitology* **121**, 227–235.
- KWIATKOWSKI, D. (1995). Malarial toxins and the regulation of parasite density. *Parasitol. Today* **11**, 206–212.
- KWIATKOWSKI, D. & NOWAK, M. (1991). Periodic and chaotic host–parasite interactions in human malaria. *Proc. Natl Acad. Sci. U.S.A.* **88**, 5111–5113.
- LELL, B., BRANDTS, C. H., GRANINGER, W. & KREMSNER, P. G. (2000). The circadian rhythm of body temperature is preserved during malarial fever. *Wien. Klin. Wochenschr.* **112**, 1014–1015.
- LELL, B., SOVRIC, M., SCHMID, D., LUCKNER, D., HERBICH, K., LONG, H. Y., GRANINGER, W. & KREMSNER, P. G. (2001). Effect of antipyretic drugs in children with malaria. *Clin. Infect. Dis.* **32**, 838–841.
- LLOYD, A. L. (2001a). The dependence of viral parameter estimates on the assumed viral lifecycle: limitations of studies of viral load data. *Proc. R. Soc. London B* **268**, 847–854.
- LLOYD, A. L. (2001b). Destabilization of epidemic models with the inclusion of more realistic distributions of infectious periods. *Proc. R. Soc. London B* **268**, 985–993.
- MOLYNEAUX, L., DIEBNER, H. H., EICHNER, M., COLLINS, W. E., JEFFREY, G. M. & DIETZ, K. (2001). *Plasmodium falciparum* parasitaemia described by a new mathematical model. *Parasitology* **122**, 379–391.
- SAUL, A. (1998). Models for the in-host dynamics of malaria revisited: errors in some basic models lead to large overestimates of growth rates. *Parasitology* **117**, 405–408.
- TRAGER, W. & JENSEN, J. B. (1976). Human malaria parasites in continuous culture. *Science* **193**, 673.
- WHITE, N. J., CHAPMAN, D. & WATT, G. (1992). The effects of multiplication and synchronicity on the vascular distribution of parasites in falciparum-malaria. *Trans. R. Soc. Trop. Med. Hyg.* **86**, 590–597.